Available online at www.sciencedirect.com
SCIENCE DIRECT
Journal of Photochemistry and Photobiology A: Chemistry 173 (2005) 13–20
Journal of Photochemistry and Photobiology A:Chemistry
www.elsevier.com/locate/jphotochem

Photocatalytic degradation of a sulfonylurea herbicide over pure and tin-doped TiO_2 photocatalysts

Fernando Fresno[a,b,*], Chantal Guillard[c], Juan M. Coronado[a], Jean-Marc Chovelon[c], David Tudela[b], Javier Soria[a], Jean-Marie Herrmann[c]

[a] *Instituto de Catálisis y Petroleoquímica, CSIC, C/Marie Curie, 2 Cantoblanco, 28049 Madrid, Spain*
[b] *Departamento de Química Inorgánica, Facultad de Ciencias, Universidad Autónoma de Madrid, Campus de Cantoblanco, 28049 Madrid, Spain*
[c] *Laboratoire d'Application de la Chimie à l'Environnement (LACE), UMR 5634, Université Claude Bernard Lyon 1, 43 Bd du 11 Novembre 1918, F-69622 Villeurbanne Cedex, France*

Received 10 September 2004; received in revised form 28 October 2004; accepted 22 December 2004
Available online 1 February 2005

Abstract

The heterogeneous photocatalytic degradation of chlorsulfuron (ChS), a sulfonylurea herbicide, has been studied using home-made Sn-doped TiO_2 samples and TiO_2 P25 from Degussa as photocatalysts. First-order kinetics were found for the disappearance of chlorsulfuron using both types of materials. Three synthesized photocatalysts were used, two of them containing 11 and 20 mass% of Sn, respectively, and one composed of pure anatase TiO_2. The sample with the lower content of tin is formed by anatase and rutile crystallites, whereas the one with a higher doping level contains anatase, rutile and SnO_2 phases. Comparison between their efficiency in the photocatalytic degradation of chlorsulfuron indicated a beneficial effect of the presence of Sn^{4+} in the TiO_2 lattice, whereas segregated SnO_2 phase induced a slower degradation of ChS when compared to pure TiO_2. However, Degussa TiO_2 P25 remains the most active material for this reaction. Based on DRIFTS and adsorption observations, an inverse dependence of the photocatalytic activity on the water adsorption capacity of the samples is proposed.

Keywords: Photocatalysis; TiO_2; Sn; Nanoparticles; Sulfonylurea herbicides; Infrared spectroscopy

1. Introduction

Heterogeneous photocatalysis has been proved to be an efficient technique for the elimination of pollutants in aqueous and gaseous media [1–4]. Its main advantages concern the large variety of pollutants which can be destroyed and the soft conditions of operation. The most commonly used photocatalyst is TiO_2, generally under the form of anatase or anatase–rutile mixtures, because of its relatively high activity, its stability under operation conditions and its low cost. When TiO_2 is irradiated with photons whose energy equals or exceeds its band gap energy, electrons (e^-) are promoted to the conduction band, leaving positive holes (h^+) in the valence band. Holes can react with hydroxyl groups on the surface of the semiconductor to produce strongly oxidizing $OH^\bullet$ radicals. On the other hand, electrons react with adsorbed molecular oxygen yielding superoxide anion radicals $O_2^{\bullet -}$. Several modifications have been attempted to increase the photoactivity of TiO_2. Significant improvement has been achieved with the use of TiO_2 nanoparticles [5,6]. In addition, the incorporation of metal ions into the TiO_2 lattice has been extensively studied as a way of increasing the TiO_2 photoactivity [7,8], whose effects are generally related to a decrease of the electron–hole recombination rate and the modification of the semiconductor band gap. In that respect, the substitution of Sn^{4+} for Ti^{4+} has led to an improvement of the photocatalytic activity of both rutile [9] and anatase [10] phases of

* Corresponding author. Tel.: +34 91 585 4775; fax: +34 91 585 4760.
E-mail address: ffresno@icp.csic.es (F. Fresno).

1010-6030/$ – see front matter © 2005 Elsevier B.V. All rights reserved.
doi:10.1016/j.jphotochem.2004.12.028

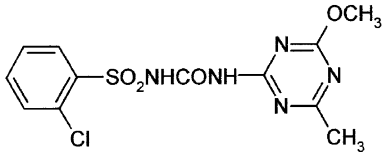

Fig. 1. Molecular structure of chlorsulfuron (ChS).

TiO_2, and $Ti_{1-x}Sn_xO_2$ nanosized photocatalysts with multiphase compositions have been recently studied for the elimination of volatile organic compounds (VOC) in the gas phase [11]. In a similar way, the presence of a second semiconductor can improve the charge separation in the photocatalytic process [12]. Particularly, the TiO_2/SnO_2 system has shown a good performance for the degradation of pollutants both in aqueous solutions [13–17] and in the gas phase [18,19]. Nevertheless, Degussa P25, which is formed by anatase and rutile in an approximately 3:1 proportion [20], remains as the standard material in photocatalysis, and it shows an especially high activity in aqueous reactions, whereas other TiO_2 based catalysts have shown better performance for reactions carried out in the gas phase [5,6,11]. In this respect, the differences between the factors affecting the photocatalytic activity of TiO_2 in gas–solid and liquid–solid reactions constitute another point of interest [21].

Sulfonylureas (Sus) constitute a recently developed class of herbicides whose chemical structure is characterized by an aryl group, a sulfonyl urea bridge and an s-triazinic ring. They are used for weed control in cereal crops [22,23]. Their broad spectrum of action with a low application dose have led, among other reasons, to a rapid acceptance of these compounds. However, their high phytotoxicity and relatively high solubility make them potential contaminants of ground waters. Recent studies [24–26] have dealt with the heterogeneous photocatalytic degradation of Sus over irradiated TiO_2 particles in aqueous suspensions, and have demonstrated the efficiency of this technique to destroy this kind of pollutants.

In this work, we have studied the photocatalytic degradation of chlorsulfuron (hereafter ChS), a sulfonylurea herbicide whose chemical structure is shown in Fig. 1, using $Ti_{1-x}Sn_xO_2$ materials and TiO_2 P25 as photocatalysts. The influence of parameters such as the irradiation flux, the presence of tin, either substituting for Ti in the TiO_2 lattice or as a segregated SnO_2 phase, in the synthesized catalysts and the different water adsorption capacity of the different samples have been studied.

2. Experimental

2.1. Materials and reagents

Chlorsulfuron (ChS) [1-(2-chlorophenylsulfonyl)-3-(4-methoxy-6-methyl-1,3,5-triazin-2-yl)urea] (99% purity) was purchased from Chem Service. ChS solutions were prepared with water from a Millipore Waters Milli-Q water purification system.

TiO_2 Degussa P25, 80% anatase–20% rutile, with a specific area of 50 $m^2\ g^{-1}$, and $Ti_{1-x}Sn_xO_2$ home-made materials were used as photocatalysts. $Ti_{1-x}Sn_xO_2$ photocatalysts were obtained by reaction of $TiCl_4$ with Ph_3SnOH in dry CH_2Cl_2 followed by thermal treatment at 723 K, as described elsewhere [11]. Commercial Ph_3SnOH (Aldrich) without further purification was used for the synthesis of the sample called TiSnA1, while Ph_3SnOH (M&T) recrystallized from ethanol was employed for the synthesis of TiSnT1. A pure TiO_2 sample (TiT), obtained by reaction of $TiCl_4$ with H_2O in CH_2Cl_2 and calcined at 723 K, was used as a reference [11].

2.2. Characterization techniques

The tin content of the doped samples was determined by X-ray fluorescence using a TXRF EXTRA-II Rich & Seifert equipment. BET surface areas were measured by N_2 adsorption at 77 K in a Micromeritics 2100 automatic apparatus. Powder XRD patterns were recorded on a Seifert XRD 3000P diffractometer using nickel-filtered Cu Kα radiation. Diffuse reflectance Fourier-transform infrared (DRIFT) spectra of the catalysts powders were obtained on a Bruker Equinox 55 equipment with a Praying Mantis diffuse reflectance device and an MCT detector, accumulating 100 scans with a 4 cm^{-1} resolution.

2.3. Photocatalytic experiments

Photocatalytic degradation reactions were carried out in a Pyrex cylindrical flask open to air with an optical window of 11 cm^2 area. The initial solution volume was 20 mL. For all experiments, TiO_2 powders were suspended in a varying concentration in the herbicide solution and the suspensions were magnetically stirred. The light source was a HPK 125 W Philips mercury UV lamp, cooled by a water circulation. The irradiation spectrum was cut-off below 340 nm with a Corning 0-52 filter in order to work in a pure photocatalytic regime with the elimination of short wavelengths able to induce side photochemical reactions. The lamp spectrum had a maximum emission at 365 nm. The light intensity could be reduced by placing metallic grids between the lamp and the reactor. The radiant flux was measured with a radiometer (United Detector Technology Inc., Model 21A power meter). Heating of the reaction suspension was avoided by including a water filter between the reactor and the lamp in order to eliminate the IR radiation.

2.4. Samples preparation

During irradiation, aliquots of the aqueous suspensions (500 μL) were collected at regular intervals and filtered through a 0.45 μm Millipore filter, in order to remove the

photocatalyst particles before analysis by an HPLC system equipped with a diode array detector (DAD).

2.5. Analytical determinations

The HPLC-DAD analyses were performed with a Varian system including a pump Prostar 230, a detector Prostar 330 and an autosampler model 410. The column was a Hypersil BDS C_{18}, 5 μm, 125 mm × 4 mm. The flow rate was 1.0 mL min^{-1} and the injection volume was 50 μL. The mobile phase was methanol (A) and water (B), whose pH was adjusted to 2.80 by using H_3PO_4. Isocratic 50% (A)–50% (B) elution conditions were used for all the analyses.

3. Results and discussion

3.1. Determination of the optimal concentration of titania photocatalyst

It is well known that the initial rates are directly proportional to the mass of catalyst (m) in heterogeneous photocatalysis, until a limit above which the reaction rates become independent of m [4]. This limit, which depends on the geometry and working conditions of the reactor, corresponds (i) to the minimal amount of photocatalyst necessary to absorb all photons, and (ii) to a full absorption of UV light. To choose this optimal quantity, the transmitted (non-absorbed) flux was measured at the exit of the photoreactor when irradiating an aqueous suspension with increasing concentrations of TiO_2 P25. Fig. 2 shows the measured irradiation flux as a function of the mass of catalyst in 20 mL of ultrapure water. As it can be seen, the absorbed light increases with increasing the amount of TiO_2 up to a limit of 35–40 mg (1.75–2 g L^{-1}). To ensure that light was optimally absorbed and that little changes in the mass of catalyst employed had no effect on the reaction rate, we chose a TiO_2 mass equal to 50 mg (2.5 g L^{-1}) for all the experiments, as chosen in previous works [25,26].

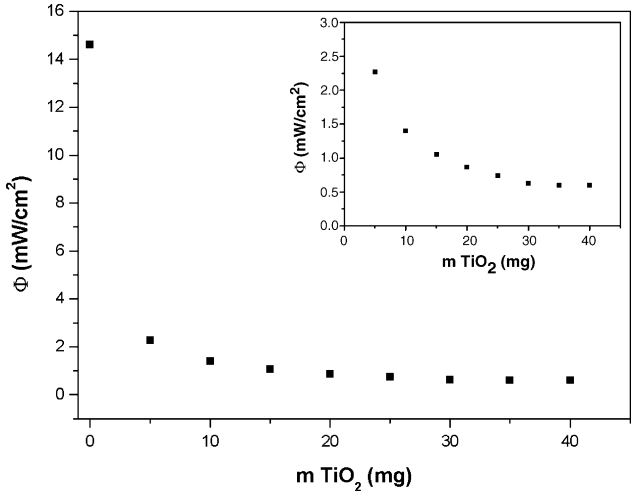

Fig. 2. Measurements of the irradiation flux (Φ) non-adsorbed by the photocatalyst and issued through from the photoreactor as a function of TiO_2 mass (m) in 20 mL of water. Inset: magnification of the plot in 0.0–3.0 mW/cm^2 range.

3.2. Adsorption of chlorsulfuron on TiO_2 in the dark

An experiment in which 50 mg of TiO_2 P25 was suspended in 20 mL of a 20 ppm aqueous solution of ChS was carried out in order to determine the time necessary to attain the equilibrium adsorption in the dark. The suspension was magnetically stirred in the absence of UV irradiation for 120 min with samples collected regularly. A decrease in the concentration of ChS until 45 min of stirring occurred, then adsorption equilibrium was attained and the concentration remained constant. Taking this into consideration, and to ensure that the adsorption equilibrium was reached, in all the experiments the TiO_2 suspension was stirred for 60 min before irradiating.

3.3. Photocatalytic degradation of ChS over TiO_2 P25

3.3.1. Degradation kinetics

Fig. 3 shows the evolution of the concentration of ChS as a function of irradiation time for the photocatalytic degradation experiment using Degussa TiO_2 P25. The photonic flux was 1.0×10^{17} photons s^{-1}. ChS disappears rapidly in the presence of irradiated P25 particles and its concentration is practically zero within 15 min. HPLC/MS experiments showed the formation of intermediates corresponding to hydroxylation of ChS by $OH^{\bullet}$ attack at different positions and to different cleavages of the sulfonylurea bridge, as it was found for other sulfonylurea herbicides in a recent work [24]. Mechanistic aspects of the degradation reaction are currently under investigation. An experiment carried out with a similar photonic flux and without the presence of TiO_2 resulted in negligible photochemical degradation.

Both first- and half-order kinetics have been proposed for the degradation of different sulfonylurea herbicides [24–26]. It has been proposed that a half kinetic order suggests a reaction in which the reactant is adsorbed in a dissociated state

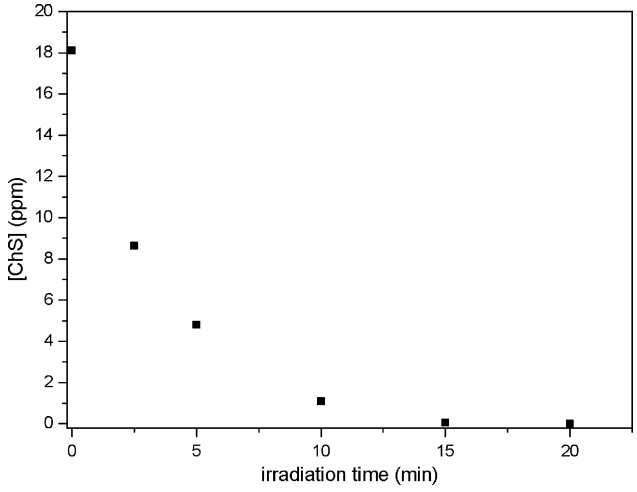

Fig. 3. Photocatalytic disappearance of ChS using TiO_2 P25.

Table 1
Linear plots for first- and half-order kinetics for the photocatalytic degradation of ChS over P25

	Slope	R^2	k
First order	0.278	0.998	$0.278 \pm 0.004\ \text{min}^{-1}$
Half order	0.35	0.958	$0.70 \pm 0.06\ \text{mol}^{1/2}\ \text{l}^{1/2}\ \text{min}^{-1}$

occupying two adsorption sites, whereas first kinetic order suggests an associative (i.e. non-dissociative) adsorption of the reactant [27,28]. Linear plots of the first four points of the reaction (where intermediate products have no significant effect on the degradation rate) were calculated considering both kinetic orders:

- For first-order kinetics, $\ln(C_0/C)$ was plotted versus time, according to the integration of the equation:

$$-\frac{dC}{dt} = k_{obs}C$$

where C is the ChS concentration and k_{obs} is the observed first-order rate constant, which is obtained as the slope in the linear plot.
- For half order kinetics, integration of the kinetic law:

$$-\frac{dC}{dt} = k_{obs}\sqrt{C}$$

results in $\sqrt{C_0} - \sqrt{C} = (1/2)k_{obs}t$, which provides k_{obs} as twice the slope of the linear representation of $\sqrt{C_0} - \sqrt{C}$ versus time.

The parameters of the linear plots obtained for both kinetic orders are listed in Table 1, as well as the observed rate constants calculated from these plots. According to the statistic parameter R^2, ChS disappearance fits better to a first kinetic order with a rate constant of $0.278 \pm 0.004\ \text{min}^{-1}$. However, it has been discussed that both associative and dissociative adsorptions can coexist on the TiO_2 surface [26]. Considering this, it is not surprising that relatively good linear regression curves are obtained for both kinetic orders.

3.3.2. Influence of the irradiation flux

Photocatalytic degradation experiments with different irradiation fluxes were carried out in order to study the influence of the photonic flux on the reaction rate. With this aim, different metallic grids were placed between the lamp and the reactor. It is well established that the rate of the photocatalytic reaction is proportional to the radiant flux until a limit above which it becomes proportional to its square root. This limit depends on the geometry and the operating conditions of the reactor, and it corresponds to the value above which electron–hole recombination becomes predominant [4]. Linear plots of $\ln(C_0/C)$ versus time for the photocatalytic degradation of ChS under three different radiant fluxes are displayed in Fig. 4, along with the calculated first-order kinetic constant (k) against the photonic flux (Φ), which are shown in the inset. As expected, the reaction rate constant increases with the increasing efficient photonic flux, and the

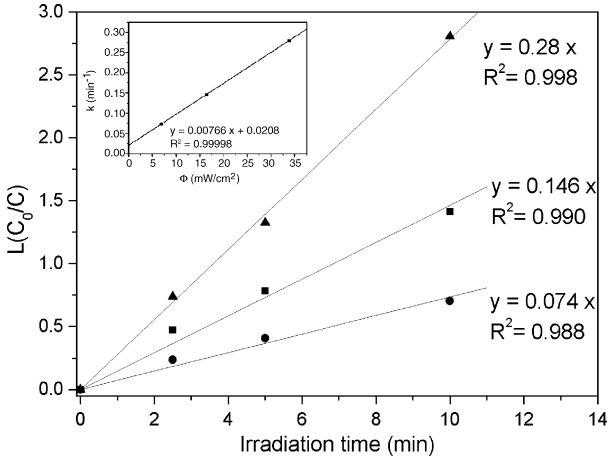

Fig. 4. Influence of the radiant flux on the photocatalytic degradation rate of ChS over TiO_2 P25. Linear plots of $\ln(C_0/C)$ vs. time for reactions under various radiant fluxes (6.9 mW/cm^2 (circles), 16.4 mW/cm^2 (squares) and 33.8 mW/cm^2 (triangles)). Inset: dependence of the calculated kinetic constant on the radiant flux.

good agreement with a linear relation between k and Φ indicates that we are working in the region where the reaction rate is directly proportional to the photonic flux. This means a true photocatalytic regime. On the other hand, the extrapolation of the linear regression curve to $\Phi = 0$ gives an intercept equal to $k = 0.02\ \text{min}^{-1}$, which would represent the value of the rate constant in the absence of UV light. This value of k, different from 0, could indicate that there exists a hydrolysis of the sulfonylurea heterogeneously catalyzed by TiO_2 in the absence of UV irradiation. The surface acidity of TiO_2 has been employed to catalyze different organic and inorganic transformations [29], and this acidity may be strong enough to catalyze the hydrolysis reaction.

3.4. Photocatalytic degradation of ChS using $Ti_{1-x}Sn_xO_2$ photocatalysts

3.4.1. Characteristics of the $Ti_{1-x}Sn_xO_2$ photocatalysts

Table 2 resumes the structural and morphological properties of the tin-doped TiO_2 photocatalysts compared to those of Degussa P25. Three different materials, with varying Sn content and phase composition were used for this study. The Sn content varies from 0 in the reference sample TiT up to

Table 2
Properties of the employed photocatalysts

Sample	Sn (mass%)	BET surface area (m^2/g)	Crystal phases	Particle size (nm)
TiSnA1	20	41	Anatase	26
			Rutile	6
			SnO_2	5
TiSnT1	11	36	Anatase	29
			Rutile	6
TiT	–	47	Anatase	16
Degussa P25	–	44	Anatase	26
			Rutile	34

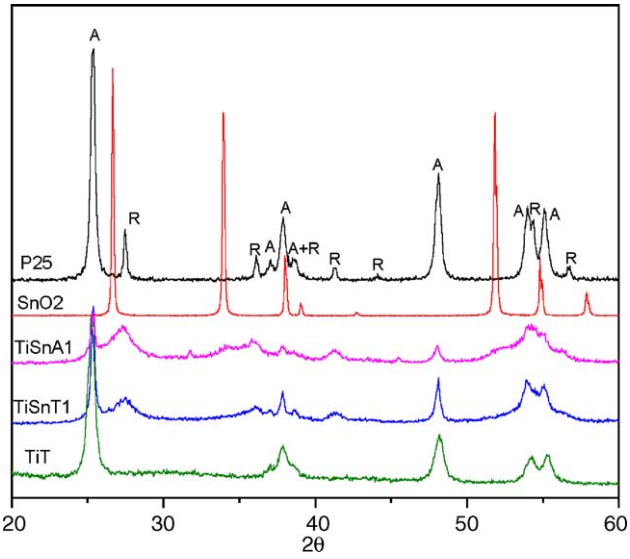

Fig. 5. XRD patterns of Degussa P25, SnO_2 (Probus) and $Ti_{1-x}Sn_xO_2$ samples (A: anatase, R: rutile).

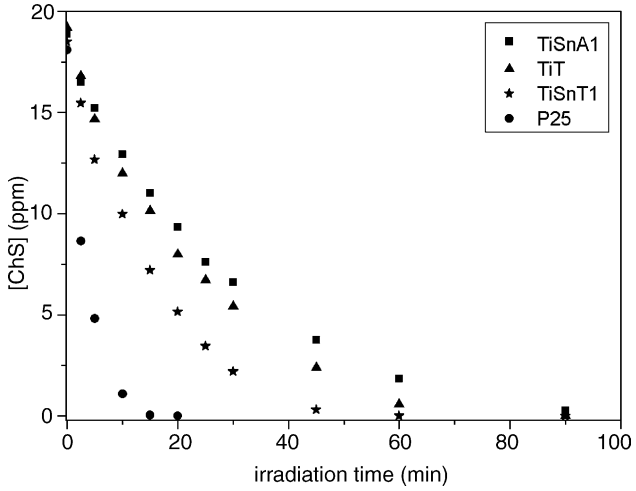

Fig. 6. Photocatalytic disappearance of ChS over the tin-doped and reference pure TiO_2 materials. Results obtained over Degussa P25 are shown for comparison.

20 wt.% in TiSnA1, as determined by TXRF. Fig. 5 shows the X-ray diffraction patterns of the tin-doped samples compared to those of TiO_2 P25 and SnO_2. The phase composition varies with the increasing content of Sn. In this respect, the pure TiO_2 reference sample is constituted of pure anatase phase, in accordance with other TiO_2 photocatalysts obtained by the same crystallization route from different precursors [5]. On the other hand, the samples containing Sn show a multiphase composition. The TiSnT1 catalyst is composed of crystallites of both anatase and rutile phases. The formation of rutile phase at a low calcination temperature is induced by the presence of Sn, as reported previously [11,30]. No SnO_2 phase is detected, which suggests the incorporation of Sn^{4+} into the TiO_2 lattice. In contrast, the TiSnA1 photocatalyst is a mixture of anatase, rutile and SnO_2 (cassiterite) phases. In the case of this sample, the suppression of the recrystallization treatment of the starting Ph_3SnOH reagent has led to both an increment of the Sn content and the formation of the cassiterite phase, which can be related to the presence of Ph_2SnO, an insoluble polymer, in the commercial reagent [31]. The BET surface areas of the prepared samples are similar and comparable to that of P25, as it can be seen in Table 2. Therefore, surface area will not determine the differences in photocatalytic activity between the different samples.

3.4.2. Degradation kinetics

Fig. 6 shows the evolution of the ChS concentration with irradiation time in the presence of the $Ti_{1-x}Sn_xO_2$ photocatalysts, compared to those obtained with TiT and with TiO_2 Degussa P25. The linear regressions of $\ln(C_0/C)$ and $\sqrt{C_0} - \sqrt{C}$ as a function of irradiation time, obtained from the first four points of the reaction, are shown in Table 3. The correlation coefficients were slightly better in all cases for first-order than for half order kinetics. On this basis, a pseudo-first-order reaction rate was considered for the photocatalytic degradation with these photocatalysts, as it was also determined for P25. Therefore, no change in the reaction rate order was observed when changing the photocatalyst, and thus the same type of adsorption should be expected in all cases. Probably both associative and dissociative adsorption occur as discussed in the reaction over irradiated P25.

Table 3 also shows the calculated first-order rate constants for TiT, TiSnT1 and TiSnA1. Although none of the tin-doped photocatalysts reaches the activity of P25, their comparison gives significant differences. The tin-doped sample TiSnT1 shows a substantially higher photocatalytic activity than TiT. Comparing these two samples, we can conclude that the presence of Sn^{4+} substituting for Ti^{4+} is improving the photocatalytic activity of TiO_2 for the reaction considered here. It has been reported that partial substitution of Sn^{4+} for Ti^{4+} has led to an increase in the photocatalytic activity of anatase for the degradation of a textile dye in aqueous solution [10], and the rutile form of TiO_2 has been doped with Sn^{4+} cations resulting in a better photocatalytic activity for the oxidation of acetone in air [9]. Similar results have been obtained with the samples employed here for the photocatalytic degradation of methylcyclohexane in an oxygen stream [11]. The presence of different crystalline phases or semiconductors has been invoked to be a factor improving the charge separation during the photocatalytic process, as has been discussed

Table 3
Linear plots of $\ln(C_0/C)$ and $\sqrt{C_0} - \sqrt{C}$ vs. time and calculated first-order rate constants for the synthesized photocatalysts compared to those for P25

Sample	Slope		R^2		k (min^{-1})
	First order	Half order	First order	Half order	
TiT	0.048	0.097	0.991	0.981	0.048 ± 0.001
TiSnT1	0.065	0.122	0.981	0.962	0.065 ± 0.003
TiSnA1	0.040	0.079	0.974	0.961	0.040 ± 0.002
P25	0.278	0.35	0.998	0.958	0.278 ± 0.004

for TiO_2(anatase)/TiO_2(rutile) [12] and TiO_2(anatase)/SnO_2 [18,19] materials, and this has been proposed to be a key factor to explain the high activity of Degussa P25 [20]. However, the previous studies of the samples presented here show that TiSnT1, constituted by anatase and rutile, as well as the reference sample TiT, formed by anatase, have better activity than P25 for the photocatalytic degradation of methylcyclohexane in the gas phase [11]. Considering this, the presence of different crystalline phases cannot be considered to be the unique reason of this improved photoactivity in the gas phase. Besides, electronic modifications induced by the presence of Sn^{4+} can lead to a larger energetic difference between the valence and conduction bands, which can result in a higher redox potential of the photogenerated carriers [9,32]. In addition, indirect band gap transitions, which are less prone to recombination, have been reported for Sn-doped TiO_2 [32]. These processes are probably related to the improved photocatalytic activity of $Ti_{1-x}Sn_xO_2$ nanoparticles. Nevertheless, the different factors influencing gas phase and solution reactions, like pH, light intensity distribution and adsorption capacity of the target molecule, make that conclusions obtained from gaseous reactions cannot be directly extrapolated to aqueous solutions.

On the other hand, the sample TiSnA1 has led to a slower photocatalytic degradation than both TiSnT1 and TiT. This indicates that the presence of a segregated SnO_2 phase, contrary to the substitution of Sn^{4+} for Ti^{4+}, has a negative effect on the photocatalytic activity of the studied samples. There exist several studies in the literature reporting a better photocatalytic performance of TiO_2/SnO_2 coupled oxides with respect to TiO_2 [13–17]. This improvement in activity has been related to a higher charge separation efficiency due to the contact between different semiconductors. It has also been reported that the preparation method of TiO_2/SnO_2 coupled oxides strongly influences their photocatalytic activity, in such a way that the presence of SnO_2 is not always positive, since an efficient contact between phases is required to achieve charge separation [16]. Besides, as the photocatalytic activity of SnO_2 itself is lower than that of TiO_2 [33], the presence of SnO_2 as a segregated phase can negatively affect the activity of the photocatalysts by decreasing the more active TiO_2 surface available for the reactants. With respect to the TiSnA1 sample, HPLC/MS experiments revealed, in contrast to the case of P25, the formation of intermediates with a higher molecular weight than the initial product, which suggests possible coupling reactions between the radicals formed upon cleavage of ChS. Therefore, a different reaction mechanism with respect to P25 is possible. Mechanistic aspects of the degradation of ChS over TiSnA1 and TiO_2 P25 will be discussed on a forthcoming publication.

3.5. Relation between adsorption of reactants and photocatalytic activity

Fig. 7 shows the relation between the percentage of ChS adsorption before irradiation, with respect to the initial concentration, and the photocatalytic degradation rate constants for the different catalysts. An increase in the kinetic constant with the increasing amount of ChS adsorbed in the dark is observed, except for the sample TiSnA1. This trend suggests that a higher adsorption of chlorsulfuron in the dark leads to a faster photocatalytic reaction. The deviation observed for TiSnA1 can be explained considering that, as discussed above, part of the surface of this catalyst can be formed of the less photocatalytically active SnO_2 phase.

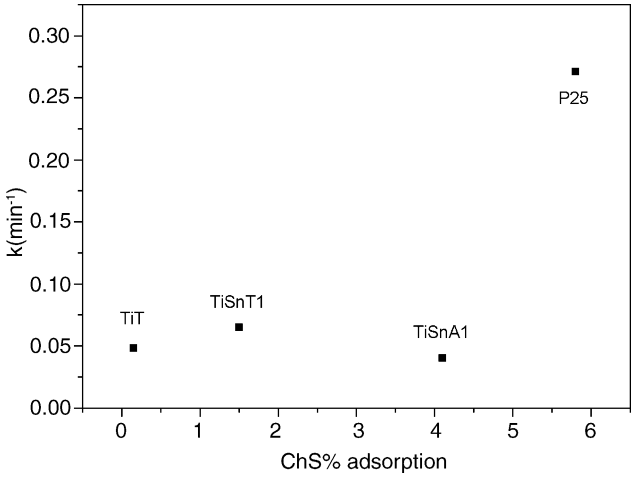

Fig. 7. Chlorsulfuron photocatalytic degradation rate constant vs. percentage of adsorption in the dark.

Water plays an important role in photocatalysis, as it is necessary for the formation of active hydroxyl radicals and its presence in gas phase photocatalytic reactions can contribute to the regeneration of active sites and to the inhibition of deactivation mechanisms [5,34]. On the other hand, the formation of a water layer on the catalyst surface can also have a detrimental effect on the photocatalytic process, by hampering the access to the active sites of the catalyst, not only for the organic reactants, [6,34,35], but also for oxygen molecules [36]. In order to gain information about the amount of water covering the samples surface, DRIFT spectra of the fresh catalysts were recorded. Basically, the monolayer of adsorbed water on the catalyst surface is considered to correspond to the first surface hydration layer in gas–solid and liquid–solid photocatalytic reactions [21], and thus this differences in the adsorbed water on the fresh powder catalysts can be related to their behaviour in the aqueous suspensions employed for the reactions. Fig. 8 shows the 4000–2500 cm^{-1} region of these spectra, in which the O–H stretching vibration mode appears. The spectra of the four samples show a weak narrow band around 3695 cm^{-1}, which has been assigned to the ν_{OH} vibration mode of the non-hydrogen-bonded (Hb) proton of assymetrically Hb water molecules, the Hb proton contributing to the intense and broad band, with maxima arising from different contributions, which appears in the 3650–2500 cm^{-1} range [37]. A band at 3200 cm^{-1} has been associated to ice-like bond ordered water clusters, while another one at 3450 cm^{-1} is indicative of bond disordered water

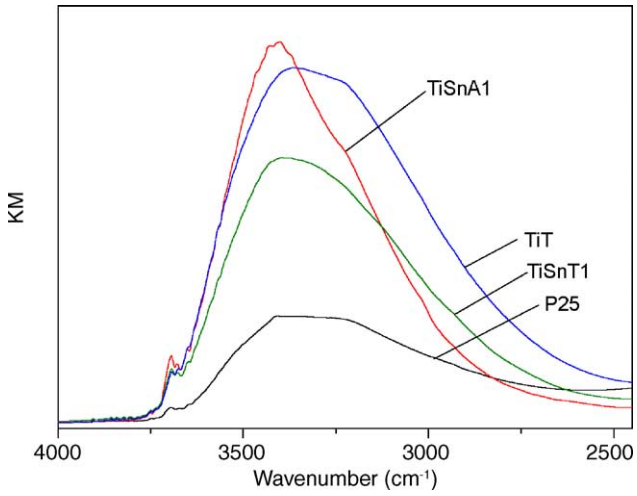

Fig. 8. Diffuse reflectance infrared spectra of the studied samples in the 2500–4000 cm^{-1} region.

clusters [38]. As it has been discussed in experimental and theoretical studies, the structure and the intermolecular interactions of the adsorbed water layers depend on the structural and surface properties of the substrate [39,40]. The shape of the ν_{OH} broad absorption observed in the DRIFT spectra of P25, TiSnT1 and TiT, formed uniquely by TiO_2 structures, is similar, while the sample TiSnA1, in which an additional SnO_2 phase is present, shows a different band shape, with a decrease in the relative contribution of bond ordered water clusters. This difference can be regarded as a reflection of modifications induced by the presence of segregated SnO_2. As it can be seen from the ν_{OH} band intensities in Fig. 8, the amount of water adsorbed on the catalysts surface increases in the order P25 < TiSnT1 < TiT. This is the opposite trend to that found for the ChS adsorption capacity (see Fig. 7) and, therefore, the kinetic constants obtained for the photocatalytic degradation of ChS increase as the ν_{OH} band intensities decrease for the samples formed by TiO_2 structures. P25 shows a big difference in the amount of adsorbed water that corresponds to the large difference in efficiency observed in the photocatalytic experiments. TiSnT1 and TiT display slightly different peak intensities, corresponding the lowest one to TiSnT1, which shows better photocatalytic performance in the degradation of chlorsurfuron. The above discussion does not refer to TiSnA1, which, as discussed above, possesses different surface properties due to the presence of SnO_2 and does not allow a direct comparison to the other samples.

These results suggest a negative influence of the water adsorption capacity of the catalysts on their photocatalytic activity for this reaction. This negative effect can be explained as a competition of water with chlorsulfuron and oxygen for the adsorption on the TiO_2 surface. In the aqueous suspension, the TiO_2 surface is completely surrounded by water molecules, and a lower capacity to adsorb water molecules or, in other words, a higher hydrophobicity of this surface, would result in a higher facility for the organic pollutant and oxygen molecules to reach the TiO_2 surface, to adsorb on it and to react, thus leading to a faster photocatalytic reaction. This can be one of the factors leading to the high photocatalytic activity of Degussa P25 in aqueous suspensions, which on the other hand has been frequently improved in the gas phase [5,6,11]. Comparing samples TiSnT1 and TiT, the incorporation of Sn^{4+} ions into the TiO_2 lattice can modify the surface characteristics of the material [9], thus leading to a higher hydrophobicity and a faster adsorption of the organic reactant molecules in aqueous suspensions.

4. Conclusions

The photocatalytic degradation of chlorsulfuron over irradiated TiO_2 P25 follows apparent first-order kinetics with a kinetic constant of 0.278 min^{-1}. The reaction rate is directly proportional to the irradiation flux, indicating a true photocatalytic regime. When using home-made tin-doped TiO_2 photocatalysts, the reaction order remains the same, but the kinetic constants are considerably lower than that obtained with P25. However, comparison of the tin-doped catalysts with a reference TiO_2 sample indicates that incorporation of Sn^{4+} into the TiO_2 lattice improves its photocatalytic activity. On the other hand, the presence of segregated SnO_2 results in a slower photocatalytic reaction. A DRIFT study suggests an inverse dependence of the photocatalytic activity of the different catalysts on their water adsorption capacity.

Acknowledgements

This study has received financial support from the project MAT2001-2112-C02-01. FF thanks the Spanish Ministerio de Ciencia y Tecnología for the financial support of a stay in LACE within his doctoral grant.

References

[1] D.F. Ollis, H. Al-Ekabi (Eds.), Photocatalytic Purification and Treatment of Water and Air, Elsevier, Amsterdam, 1993.
[2] M. Schiavello (Ed.), Photocatalysis and Environment: Trends and Applications, NATO ASI Series C, vol. 238, Kluwer Academic Publishers, London, 1987.
[3] M.R. Hoffmann, S.T. Martin, W. Choi, D. Bahnemann, Chem. Rev. 95 (1995) 69–96.
[4] J.M. Herrmann, Catal. Today 53 (1999) 115–129.
[5] A.J. Maira, K.L. Yeung, J. Soria, J.M. Coronado, C. Belver, C.Y. Lee, V. Augugliaro, Appl. Catal. B: Environ. 29 (2001) 327–336.
[6] L. Cao, A. Huang, F.-J. Spiess, S.L. Suib, J. Catal. 188 (1999) 48–57.
[7] W. Choi, A. Termin, M.R. Hoffmann, J. Phys. Chem. 98 (1994) 13669–13679.
[8] M. Anpo, Stud. Surf. Sci. Catal. 130 (2000) 157–166.
[9] J. Lin, J.C. Yu, D. Lo, S.K. Lam, J. Catal. 183 (1999) 368–372.
[10] S.K. Zheng, T.M. Wang, W.C. Hao, R. Shen, Vacuum 65 (2002) 155–159.
[11] F. Fresno, J.M. Coronado, D. Tudela, J. Soria, Appl. Catal. B: Environ. 55 (2005) 159–167.

[12] T. Kawahara, Y. Konishi, H. Tada, N. Tohge, J. Nishii, S. Ito, Angew. Chem. Int. Ed. Engl. 41 (2002) 2811–2813.
[13] K. Vinodgopal, P.V. Kamat, Environ. Sci. Technol. 29 (1995) 841–845.
[14] K. Vinodgopal, I. Bedja, P.V. Kamat, Chem. Mater. 8 (1996) 2180–2187.
[15] L. Shi, C. Li, H. Gu, D. Fang, Mater. Chem. Phys. 62 (2000) 62–67.
[16] J. Yang, D. Li, X. Wang, X. Yang, L. Lu, J. Solid State Chem. 165 (2002) 193–198.
[17] Y. Cao, X. Zhang, W. Yang, H. Du, Y. Bai, T. Li, J. Yao, Chem. Mater. 12 (2000) 3445–3448.
[18] H. Tada, A. Hattori, Y. Tokihisa, K. Imai, N. Tohge, S. Ito, J. Phys. Chem. B 104 (2000) 4585–4587.
[19] T. Kawahara, Y. Konishi, H. Tada, N. Tohge, S. Ito, Langmuir 17 (2001) 7442–7445.
[20] T. Ohno, K. Sarukawa, K. Tokieda, M. Matsumura, J. Catal. 203 (2001) 82–86.
[21] G. Marci, M. Addamo, V. Augugliaro, S. Coluccia, E. García-López, V. Loddo, G. Martra, L. Palmisano, M. Schiavello, J. Photochem. Photobiol. A: Chem. 160 (2003) 105–114.
[22] H.M. Brown, Pestic. Sci. 29 (1990) 263–281.
[23] H.M. Brown, J.C. Cotterman, Recent advances in sulfonyurea herbicides, in: J. Stetter, W. Ebing (Eds.), Chemistry of Plant Protection—Herbicides Inhibiting Branch Chained Amino Acid Biosynthesis, vol. 10, Springer-Verlag, Berlin, 1994, pp. 47–81.
[24] V. Maurino, C. Minero, E. Pelizzetti, M. Vincenti, Colloids Surf. A: Physicochem. Eng. Aspects 151 (1999) 329–338.
[25] E. Vulliet, C. Emmelin, J.M. Chovelon, C. Guillard, J.M. Herrmann, Appl. Catal. B: Environ. 38 (2002) 127–137.
[26] E. Vulliet, J.M. Chovelon, C. Guillard, J.M. Herrmann, J. Photochem. Photobiol. A: Chem. 159 (2003) 71–79.
[27] P. Pichat, J.M. Herrmann, J. Disdier, H. Courbon, M.N. Mozzanega, N. J. Chim. 5 (1981) 627–636.
[28] A. Marinas, C. Guillard, J.M. Marinas, A. Fernández, A. Agüera, J.M. Herrmann, Appl. Catal. B: Environ. 34 (2001) 241–252.
[29] I. Salem, Catal. Rev. Sci. Eng. 45 (2003) 205–296.
[30] K.N.P. Kumar, K. Keizer, A.J. Burgraaf, T. Okubo, J. Nagamoto, J. Mater. Chem. 3 (1993) 923–929.
[31] R. West, R.H. Baney, D.L. Powell, J. Am. Chem. Soc. 82 (1960) 6269.
[32] F.R. Sensato, R. Custodio, E. Longo, A. Beltran, J. Andrés, Catal. Today 85 (2003) 145–152.
[33] L. Cao, F.-J. Spiess, A. Huang, S.L. Suib, J. Phys. Chem. B 103 (1999) 2912–2917.
[34] H. Einaga, S. Futamura, T. Ibusuki, Appl. Catal. B: Environ. 38 (2002) 215–225.
[35] D.S. Muggli, M.J. Backes, J. Catal. 209 (2002) 105–113.
[36] M.A. Henderson, W.S. Epling, C.H.F. Peden, C.L. Perkins, J. Phys. Chem. B 107 (2003) 534–545.
[37] L.F. Scatena, M.G. Brown, G.L. Richmond, Science 292 (2001) 908–912.
[38] Q. Du, E. Freysz, Y.R. Shen, Phys. Rev. Lett. 72 (1994) 238–241.
[39] P.A. Thiel, T.E. Madey, Surf. Sci. Rep. 7 (1987) 211–385.
[40] A. Tilocca, A. Selloni, J. Phys. Chem. B 108 (2004) 4743–4751.